2024 European Control Conference (ECC)
June 25-28, 2024. Stockholm, Sweden

Communication-aware formation control for networks of AUVs

Simon A. Hoff[1], Josef Matouš[1], Damiano Varagnolo[1], and Kristin Y. Pettersen[1]

Abstract— **We propose a distributed formation control algorithm augmented with channel awareness. We consider autonomous underwater vehicles (AUVs) that are able to communicate over an acoustic link using a Time Division Multiple Access (TDMA) protocol, and to measure the Signal-to-Noise Ratio (SNR) of incoming messages. Based on the measured SNR and packet loss, we endow them with a distributed formation control scheme that accounts for the time-varying nature of the acoustic communication channel. This scheme allows a network of N AUVs to follow a pre-determined, twice-differentiable path while adapting their formation. The size of the formation is dynamically scaled by a formation adaptation mechanism to stabilize the estimated packet loss probability at a desired level. A distributed packet loss estimator is then built on top of the same average consensus routines used by the formation control algorithm, and thus comes with a minimal communication overhead. We test the algorithm by means of high-fidelity simulators, and verify its efficacy in making the network of agents retain formation-wide communication capabilities in a range of cases.**

I. Introduction

Autonomous underwater vehicles (AUVs) are increasingly being used for several applications, such as seabed mapping, environmental monitoring, and search-and-rescue missions. Most such operations are performed with only one vehicle, but this may implicitly drive up mission costs. Indeed AUVs typically require expensive support vessels to stay nearby between deployment and retrieval. Multiple AUVs cooperatively solving the task may significantly reduce mission duration, and thereby the total mission cost.

Establishing autonomous cooperative underwater operations is a challenging task, especially due to the complexity of exchanging information in the underwater realm. In several applications (e.g., seabed mapping) the average distance between the AUVs must be at minimum in the order of tens of meters, something that excludes all means of inter-AUV information exchange but acoustic communications.

The control algorithms that make AUVs coordinate should thus be designed to account for the time variability of acoustic communications. Generally, such controllers should be adaptive, maximizing performance while maintaining acceptable information exchange between the AUVs.

This work was partly supported by the Research Council of Norway through project No. 302435 and the Centres of Excellence funding scheme, project No. 223254.

[1]Simon A. Hoff, Josef Matouš, Damiano Varagnolo, and Kristin Y. Pettersen are with the Department of Engineering Cybernetics, Norwegian University of Science and Technology, Trondheim, Norway {simon.a.hoff, josef.matous, damiano.varagnolo, kristin.y.pettersen}@ntnu.no

In this paper, we seek to introduce communication awareness in formation control schemes by adjusting the formation size. In other words, we are aiming to maximize inter-agent distance while maintaining a prescribed packet loss.

Literature review: The null-space-based (NSB) behavior algorithm is well suited to tackling the cooperative formation path-following problem due to the ability to design the goals such as formation keeping and path following as independent tasks. This was investigated by [1]–[3], and then further extended by [4], [5]. These solutions all have the shortcoming that they are centralized, meaning that they rely on a perfect communication link. Conversely, the acoustic communication found in underwater vehicles is not perfect, suffering from both latency and packet losses. In [6] this was addressed by making the algorithm distributed, proving stability under perfect communication conditions, and demonstrating experimentally that the algorithm works even for realistic conditions with acoustic communication.

Based on this approach we seek to find ways to adapt the formation to the communication conditions. There have been several efforts made to estimate the acoustic communication channel for motion planning purposes. In [7], a high-efficiency estimator for acoustic communication channels was proposed. In [8], high-fidelity acoustic simulations were used to determine areas where a reliable acoustic link could be maintained. However, this work relies on one side of the acoustic link being fixed, making it less suitable for a situation where both transmitter and receiver are moving relative to the environment. In [9], acoustic communication conditions were predicted using a combination of physical modeling and learning. As the work of [8], this is still based on one end of the acoustic link being fixed, making it less applicable for multi-agent systems.

In [10] integral reinforcement learning was used to estimate the properties of the communication channel and perform communication-aware formation control with the estimates. In that case, there is no direct communication between AUVs, but rather between the AUVs and several fixed buoys.

In [11] distributed model predictive control (MPC) was used to plan paths over long horizons while maintaining connectivity in the swarm. Their approach allows for flexibility both in the sense that full connectivity is not required, but also in that the AUVs are only required to be within range when communications are happening. A disadvantage of MPC is however that it requires significant computational resources compared to reactive control methods such as the NSB-based method presented in this paper.

Statement of contributions: We introduce communication awareness into AUV formation control, making the formation adapt to changing communication conditions, to maximize performance while retaining a minimum connectivity. Specifically we propose a method for scaling the AUV formation by extending the distributed NSB algorithm described in [6], taking into account each vehicle's perception of the communication channel and the associated packet loss. The method has very low computational and communication overhead, as there is no need for simulation of the communication channel on board the vehicles, and only two values need to be communicated between agents. The method is tested in high-fidelity simulations.

Structure of the manuscript: We first define the problem to be solved in Sec. II. Then we present the control system employed in Sec. III. We present the simulation setup used in Sec. IV, and corresponding results and discussion in Sec. V. Finally we present concluding remarks and suggestions for future work in Sec. VI.

II. Problem definition

We consider N AUVs tasked with following a predetermined, twice differentiable path. The AUVs are able to communicate over an acoustic link using a time division multiple access (TDMA) protocol. The acoustic modems are assumed to measure the signal-to-noise ratio (SNR) of incoming messages.

This paper aims to enable the AUVs to scale the formation in response to changing communication conditions in order to stabilize the packet loss below a pre-determined rate, under the assumption that the AUVs are able to navigate perfectly without any errors accumulating.

III. Formation path-following

In this section, we will first introduce the centralized NSB algorithm of [4], [5] which solves the formation path following problem when the communication channel is perfect. Then we will summarize the distributed NSB algorithm of [6] which extends the centralized version to handle imperfect communication in the sense that communication is only done at certain times (discretization), and there is both latency and possibility of packet loss present. Finally, we present a novel algorithm that extends [4], [5] and [6], letting the formation autonomously scale to maximize inter-agent distance, i.e. coverage, while maintaining a prescribed packet loss.

To explain the distributed NSB algorithm, we first need to define the formation path-following problem and introduce the centralized version, as shown in [4], [5].

Consider a fleet of N vehicles. The position of vehicle i is given by $\mathbf{p}_i \in \mathbb{R}^3$. We assume that the vehicle can be modeled as a single-integrator system, *i.e.*, $\dot{\mathbf{p}}_i = \mathbf{v}_i$, where $\mathbf{v}_i \in \mathbb{R}^3$ is the input velocity. Let $\mathbf{p}_p : \mathbb{R} \mapsto \mathbb{R}^3$ be a function that represents the desired path. We assume that $\mathbf{p}_p$ is $\mathcal{C}^2$ and regular, *i.e.*, that it is continuously differentiable up to its second partial derivative, and its first partial derivative satisfies $\left\| \frac{\partial \mathbf{p}_p(s)}{\partial s} \right\| \neq 0$, for all $s \in \mathbb{R}$. If a path is regular, then there exists a so-called *path-tangential* coordinate frame, and a corresponding rotation matrix $\mathbf{R}_p$ (see Fig. 1). Moreover, if a path is $\mathcal{C}^2$, then the partial derivative of $\mathbf{R}_p$ with respect to the path parameter s exists and is continuous.

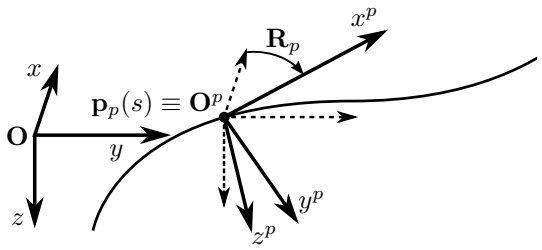

Fig. 1. Illustration of the path-tangential coordinate frame. $\mathbf{O}$ denotes the origin of the inertial coordinate frame, $\mathbf{O}^p$ denotes the origin of the path-tangential coordinate frame.

Let $\mathbf{p}_b = \frac{1}{N}\sum_{i=1}^{N} \mathbf{p}_i$ denote the barycenter of the fleet. Then, the goal of path-following is to control the vehicles so that $\mathbf{p}_b \to \mathbf{p}_p(s)$.

The goal of formation keeping is to control the relative positions of the vehicles. We assume that the desired formation should rotate with the desired path. In other words, the vehicles should be controlled so that $\mathbf{p}_i - \mathbf{p}_b \to \mathbf{R}_p \mathbf{p}^f_{f,i}$, where $\mathbf{p}^f_{f,i} \in \mathbb{R}^3$ represents the desired position of vehicle i in the formation. Note that the relative positions of the vehicles satisfy

$$\sum_{i=1}^{N} \mathbf{p}_i - \mathbf{p}_b = \mathbf{0}. \tag{1}$$

Consequently, to make the formation-keeping problem feasible, the desired formation vectors must satisfy

$$\sum_{i=1}^{N} \mathbf{p}^f_{f,i} = \mathbf{0}. \tag{2}$$

A. The centralized NSB algorithm

The following section will summarize the results of [4], [5], describing the centralized NSB algorithm.

In a centralized NSB algorithm, the desired behavior of the system is expressed as a hierarchy of tasks (for more information, the reader is referred to [12]). To solve the formation path-following problem, two tasks are defined: formation keeping and path following. The variables associated with the formation-keeping and path-following tasks are denoted by lower indices f and p, respectively. The *task variables* $\boldsymbol{\sigma}_f$ and $\boldsymbol{\sigma}_p$ that describe these two tasks are given by

$$\boldsymbol{\sigma}_f = \begin{bmatrix} \mathbf{p}_1 - \mathbf{p}_b \\ \vdots \\ \mathbf{p}_N - \mathbf{p}_b \end{bmatrix}, \qquad \boldsymbol{\sigma}_p = \mathbf{p}_b. \tag{3}$$

To simplify further notation, let $\mathbf{p} = \left[\mathbf{p}_1^{\mathrm{T}}, \ldots, \mathbf{p}_N^{\mathrm{T}}\right]^{\mathrm{T}}$ and $\mathbf{v} = \left[\mathbf{v}_1^{\mathrm{T}}, \ldots, \mathbf{v}_N^{\mathrm{T}}\right]^{\mathrm{T}}$ denote the concatenated position and velocity vectors of the vehicles. The time derivatives of the task variables are then given by

$$\dot{\boldsymbol{\sigma}}_f = \mathbf{J}_f \mathbf{v}, \qquad \dot{\boldsymbol{\sigma}}_p = \mathbf{J}_p \mathbf{v}, \tag{4}$$

where $\mathbf{J}_f = \frac{\partial \boldsymbol{\sigma}_f}{\partial \mathbf{p}}$ and $\mathbf{J}_p = \frac{\partial \boldsymbol{\sigma}_p}{\partial \mathbf{p}}$ are the Jacobian matrices of the tasks.

Let $\dot{\boldsymbol{\sigma}}_f^*$ and $\dot{\boldsymbol{\sigma}}_p^*$ denote the desired closed-loop behavior of the two tasks. Then, the input velocities $\mathbf{v}_f$ and $\mathbf{v}_p$ that achieve this behavior are given by

$$\mathbf{v}_f = \mathbf{J}_f^\dagger \dot{\boldsymbol{\sigma}}_f^*, \qquad \mathbf{v}_p = \mathbf{J}_p^\dagger \dot{\boldsymbol{\sigma}}_p^*, \tag{5}$$

where $\mathbf{A}^\dagger$ is the Moore-Penrose pseudoinverse. To combine the two input velocities, the null-space projection is used. Assuming that the formation-keeping task has a higher priority, the combined input velocity is given by

$$\mathbf{v} = \mathbf{v}_f + \left(\mathbf{I} - \mathbf{J}_f^\dagger \mathbf{J}_f\right) \mathbf{v}_p. \tag{6}$$

To solve the formation path-following problem, the following control laws for $\dot{\boldsymbol{\sigma}}_f^*$ and $\dot{\boldsymbol{\sigma}}_p^*$ were proposed

$$\dot{\boldsymbol{\sigma}}_f^* = \dot{\boldsymbol{\sigma}}_{f,d} - k_f \left(\boldsymbol{\sigma}_f - \boldsymbol{\sigma}_{f,d}\right), \tag{7}$$

$$\dot{\boldsymbol{\sigma}}_p^* = \mathbf{v}_{\mathrm{LOS}}, \tag{8}$$

where $\boldsymbol{\sigma}_{f,d} = \left[(\mathbf{R}_p \mathbf{p}_{f,1}^f)^{\mathrm{T}}, \ldots, (\mathbf{R}_p \mathbf{p}_{f,N}^f)^{\mathrm{T}}\right]^{\mathrm{T}}$ is the desired value of the formation-keeping task variable, k_f is a positive gain, and $\mathbf{v}_{\mathrm{LOS}}$ is a velocity vector given by a line-of-sight (LOS) guidance law. Specifically, the following LOS guidance law is employed

$$\mathbf{v}_{\mathrm{LOS}} = \frac{U_d}{D} \mathbf{R}_p \begin{bmatrix} \Delta \\ -y_b^p \\ -z_b^p \end{bmatrix}, \tag{9}$$

where $U_d > 0$ is the desired path-following speed, $D = \sqrt{\Delta^2 + (y_b^p)^2 + (z_b^p)^2}$, $\Delta > 0$ is a constant lookahead distance, and y_b^p and z_b^p is the position of the barycenter expressed in the path-tangential coordinate frame (*i.e.*, $[x_b^p, y_b^p, z_b^p]^{\mathrm{T}} = \mathbf{R}_p(\mathbf{p}_b - \mathbf{p}_p(s))$.

Note that the path parameter s can be treated as an additional "degree of freedom" in the controller design. Inspired by [13], the following update law of the path parameter was chosen

$$\dot{s} = U_d \left(\frac{\Delta}{D} + k_s \frac{x_b^p}{\sqrt{1 + (x_b^p)^2}}\right) \left\| \frac{\partial \mathbf{p}_p(s)}{\partial s} \right\|, \tag{10}$$

where k_s is a positive gain.

B. A distributed NSB algorithm

The algorithm presented in the previous section is centralized, meaning that in order to implement it in a real-life scenario there must be a central node that can communicate and coordinate with all vehicles. In this section, we summarize the results from [6], which demonstrate how to implement the formation path-following algorithm in a distributed manner.

Substituting (7) and (8) into (6), we get the following expression for the velocity input of vehicle i

$$\mathbf{v}_i = \dot{\boldsymbol{\sigma}}_{f,d,i} - k_f \left(\mathbf{p}_i - \mathbf{p}_b - \boldsymbol{\sigma}_{f,d,i}\right) + \mathbf{v}_{\mathrm{LOS}}, \tag{11}$$

where $\boldsymbol{\sigma}_{f,d,i} = \mathbf{R}_p \mathbf{p}_{f,i}^f$. We can see that in order to perform the NSB algorithm, the vehicles must have access to two "global" variables: the position of the barycenter $\mathbf{p}_b$, and the path parameter s.

To implement the distributed NSB algorithm, two "local" variables were introduced. Let $\hat{\mathbf{p}}_{b,i}$ and s_i be the estimates of the barycenter and the path parameter for vehicle i. The vehicle then calculates its input velocity as

$$\mathbf{v}_i = \dot{\boldsymbol{\sigma}}_{f,d,i} - k_f \left(\mathbf{p}_i - \hat{\mathbf{p}}_{b,i} - \boldsymbol{\sigma}_{f,d,i}\right) + \hat{\mathbf{v}}_{\mathrm{LOS},i}, \tag{12}$$

where

$$\hat{\mathbf{v}}_{\mathrm{LOS},i} = \frac{U_d}{D_i} \mathbf{R}_p \left[\Delta, -y_{b,i}^p, -z_{b,i}^p\right]^{\mathrm{T}}, \tag{13}$$

where $\left[x_{b,i}^p, y_{b,i}^p, z_{b,i}^p\right]^{\mathrm{T}} = \mathbf{R}_p \left(\hat{\mathbf{p}}_{b,i} - \mathbf{p}_p(s_i)\right)$ and $D_i = \sqrt{\Delta^2 + (y_{b,i}^p)^2 + (z_{b,i}^p)^2}$

The estimates $\hat{\mathbf{p}}_{b,i}$ and s_i are continuously updated using the following adaptation laws

$$\dot{\hat{\mathbf{p}}}_{b,i} = \hat{\mathbf{v}}_{\mathrm{LOS},i}, \tag{14}$$

$$\dot{s}_i = U_d \left(\frac{\Delta}{D_i} + k_s \frac{x_{b,i}^p}{\sqrt{1 + (x_{b,i}^p)^2}}\right) \left\| \frac{\partial \mathbf{p}_p(s_i)}{\partial s_i} \right\|. \tag{15}$$

We then assume that each vehicle broadcasts a packet consisting of $\hat{\mathbf{p}}_{b,i}$ and s_i. When vehicle i receives a packet from vehicle j, it updates its estimates using the following consensus law

$$\hat{\mathbf{p}}_{b,i}^+ = (1 - c)\hat{\mathbf{p}}_{b,i} + c\hat{\mathbf{p}}_{b,j}, \tag{16}$$

$$s_i^+ = (1 - c)s_i + cs_j, \tag{17}$$

where $c \in (0, 1)$ is a mixing gain.

C. Formation adjustment

In Sections III-A and III-B we described NSB algorithms for formation path-following in the centralized and decentralized cases. In [4]–[6], these are shown to provide stability guarantees under perfect communication conditions. However, underwater communication is very challenging, and in this section we propose a communication-aware algorithm that adjusts the formation size to maximize coverage while maintaining a minimum connectivity. Specifically, the formation adjustment algorithm aims to maximize the formation size while stabilizing the packet loss at a desired level l_d, by scaling the formation vectors $\mathbf{p}_{f,i}^f$introduced in (2) by a factor γ. As the packet loss depends directly on the SNR, this is equivalent to stabilizing the average SNR at some unknown value. The SNR is assumed to be stochastic with a slowly varying, unknown distribution. This means that the goal is to let the fraction of the distribution that falls below the critical SNR be equal to l_d.

The scaling of the formation is performed by a cascaded control design. The inner loop is primarily designed to handle changes in noise level, which will shift the entire SNR distribution. We assume that small changes to the formation scale will only shift the distribution, with minimal effect on the shape of the distribution.

In order to handle changes in ambient noise, the fleet will aim to keep the average received SNR at a reference value SNR_d. We achieve this by adjusting the formation size according to the measured SNR of incoming messages. It is important to note that no SNR measurement will be available if a message is lost. If we assume that all messages below $12\,\mathrm{dB}$ are lost, any lost message is replaced by a constant SNR, $\mathrm{SNR}_{\mathrm{loss}}$, which in this work is set equal to $12\,\mathrm{dB}$.

To scale the formation we aim to stabilize the average SNR of incoming packets at the reference value SNR_d. This average of the SNR is estimated with a moving average filter

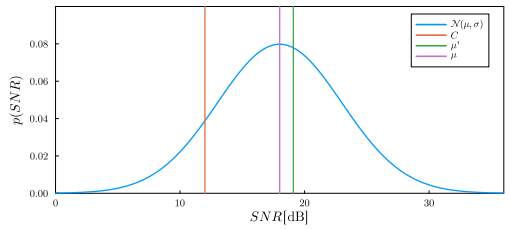

Fig. 2. Example of how a distribution truncated from one side at C leads to a biased estimate of the mean μ'.

of length L_{SNR}. Since there will be no SNR measurement for lost packets, lost packets are represented by a constant value SNR_{loss}. Under the assumption that the mean of the received SNR is equal to SNR_d, this will lead to an estimate of the mean that is higher than SNR_d, as the distribution will be truncated from one side, as shown in Figure 2. This is solved by saturating the SNR of successfully decoded packets at $2\text{SNR}_d - \text{SNR}_{\text{loss}}$. The mean deviation of the SNR of successfully decoded packets is then computed as

$$\Delta\text{SNR}_{\text{mean}} = \frac{1}{N_{\text{rec}}} \sum_{\text{SNR}_{\text{rec}}} \big(\min(\text{SNR}_{\text{rec}}, 2\text{SNR}_d - \text{SNR}_{\text{loss}}) - \text{SNR}_d\big), \tag{18}$$

with N_{rec} as the number of successfully decoded packets within a buffer time, making $\Delta\text{SNR}_{\text{mean}}$ a moving average filter.

The local formation adjustment for agent i is given by

$$\gamma_i^{new}(k) = \gamma_i(k-1) + K'_{\text{scale}}\big((1-l)\Delta\text{SNR}_{\text{mean}} - l(\text{SNR}_d - \text{SNR}_{\text{loss}})\big), \tag{19}$$

where $\gamma_i^{new}(k)$ is the formation scale proposal for agent i at time step k, and $\gamma_i(k-1)$ is the synchronized formation scale of the formation at the previous time step, from the perspective of agent i. Further, K'_{scale} is a tunable gain, and SNR_{loss} is equal to the cutoff SNR (12 dB).

By examining (19) it is clear that if SNR_d changes, so does the maximal change in formation scale per time step, which is undesirable. By normalizing the term we avoid this issue, making K_{scale} the maximal change in formation scale in any given time step:

$$\gamma_i^{\text{new}}(k) = \gamma_i(k-1) + K_{\text{scale}}\left(\frac{1-l}{\text{SNR}_d - \text{SNR}_{\text{loss}}}\Delta\text{SNR}_{\text{mean}} - l\right). \tag{20}$$

Here, $K_{\text{scale}} = K'_{\text{scale}}(\text{SNR}_d - \text{SNR}_{\text{loss}})$.

We synchronize the local scale between agents using exact dynamic minimum-consensus [14]. This ensures that the fleet operates in a risk-averse fashion, emphasizing not exceeding the prescribed packet loss as much as possible. This is particularly important since the presented control system relies heavily on consensus algorithms.

Depending on various conditions such as the sound speed profile and the bathymetric profile, the distribution of the SNR may change over time. This includes both changes to the mean and the variance of the distribution. In particular, this means that the sensitivity to small changes in formation scale may vary over time. This is handled by letting the reference value SNR_d vary with time.

In order to control the reference value SNR_d we consider the desired packet loss l_d. Similarly to how the formation is scaled, this is also performed by a form of proportional control

$$\text{SNR}_{d,i}^{\text{new}}(k) = \text{SNR}_{d,i}(k-1) + K_T\big(l_{mw,L}(k) - l_d\big), \tag{21}$$

where $\text{SNR}_{d,i}^{\text{new}}(k)$ is the new proposal for reference SNR, $\text{SNR}_{d,i}(k-1)$ is the synchronized reference SNR from the previous time step, K_T is the gain, and $l_{mw,L}(k)$ is the loss over a moving window of length L up to time step k, given by

$$l_{mw,L}(k) = \frac{1}{L}\sum_{i=k-L+1}^{k} I_{p(i)}, \tag{22}$$

where $I_{p(i)}$ is an indicator function for successful packet decoding at time step i, i.e. successfully receiving a packet. Synchronization of the local thresholds is performed using the dynamic average consensus protocol presented in [15].

It is important to note that the formation adjustment needs to have a significantly lower bandwidth than the formation control dynamics. In this case, γ can be assumed constant from the perspective of the formation control, which in turn ensures that the proofs of [4]–[6] hold. This means that convergence to the appropriate formation scale may take a long time under certain conditions. Further, the threshold adjustment needs to have a significantly lower bandwidth than the formation scaling.

An advantage of the presented method is that it requires very little communication bandwidth, which is beneficial for underwater communications where communication bandwidth is a precious and limited resource. As a whole, the presented control system only requires transmission of one 3D point, and 3 real numbers (6 real numbers total), namely $\hat{\mathbf{p}}_{b,i}$, s_i, γ_i^{new}, and $\text{SNR}_d^{\text{new}}$.

IV. Simulation Setup

This section describes the simulation setup used. The method has been tested in simulation with 3 AUVs following a circular path with radius 10 km. The vehicles are simulated as 3D unicycles, as this captures the underactuated dynamics of the AUVs adequately at the movement scales presented here. The vehicles are organized in a triangular formation, with distances 100 m from each vehicle to the barycenter, at a constant depth of 120 m.

The acoustic channel is simulated using the Ray tracer provided by the julia packages `UnderwaterAcoustics.jl` and `AcousticRayTracers.jl` [16], with a frequency of 25 kHz, and a source strength of 170 dB (relative to 1 µPa at 1 m). The sound speed profile used is from an ocean forecast for the North Sea on July 5th, 2017. from the Norwegian meteorological institute (`https://thredds.met.no`).

The bathymetric data are from outside the coast of Trøndelag, Norway, with the origin shifted to $[N, E] =$

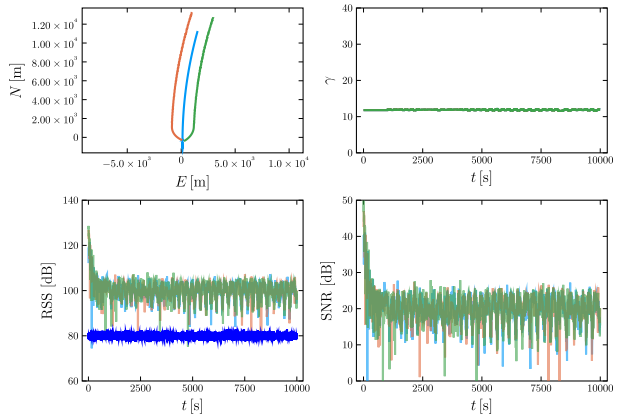

Fig. 3. Example of the system performance under the simulated environment case 1 (flat seabed and constant noise level), with 3 agents, respectively shown in light blue, orange, and green. The top left shows the trajectories of the formation, the top right shows the formation scale γ, the bottom left shows the received signal strength (RSS) as well as the noise level in dark blue, and the bottom right shows the SNR.

$[7182\,\mathrm{km}, 195\,\mathrm{km}]$ in UTM33N and were obtained from the Norwegian mapping authority (`https://dybdedata.kartverket.no/`).

To limit the time the system takes to converge, the scale is initialized using a simulation of the communication channel. This simulation assumes a flat seabed and uses an approximate sound speed profile (SSP), in this case, the average SSP for the area in the corresponding month of the preceding year.

V. Results and Discussion

In the following, we present the results of testing the presented methods in numerical simulations. The algorithm has been tested in three simulation environments:

1) a case with a flat bathymetric profile and white noise on the communication channel, to investigate how the algorithm converges in a steady-state situation,
2) a case with a random walk process to the noise level, to investigate how the algorithm is able to adjust the formation to varying noise levels (e.g., caused by a passing ship),
3) a case that mimics the more realistic conditions of varying noise levels and a non-constant bathymetric profile.

In all simulations the formation adjustment is activated after $t = 1000\,\mathrm{s}$ in order to allow the formation to stabilize and to fill the buffer with sufficiently many packets to get good estimates for the packet loss and received packet SNR. The prescribed packet loss l_d is 10% in all three cases. The tuning parameters for the communication-aware formation scaling are $K_{\text{scale}} = 0.03$ and $K_T = 0.1$. The tuning parameters for the NSB formation control algorithm are $k_f = 0.3$, $U_d = 1.3\mathrm{m\,s^{-1}}$, $\Delta = 10\,\mathrm{m}$, $c = 0.3$, and $k_s = 0.2$.

Fig. 3 shows how the algorithm is able to converge under ideal conditions, characterized by a flat seabed at depth $150\,\mathrm{m}$ and an ambient noise level of $80\,\mathrm{dB}$ with a zero mean white noise component with variance $\sigma^2 = 0.8\,\mathrm{dB}$. We note some ripples in the formation scale γ due to the presence of bursts of packets losses. These perturbations are though limited in value, and centered around a constant γ. From a statistical perspective, the amplitude of these ripples represent the level of stochasticity of the packets loss bursts. This amplitude depends on how fast the overall algorithm changes the estimated communication channel state, and this highlights the existence of intrinsic tradeoffs between the speed of convergence of this estimator and the speed of reaction induced by the NSB algorithm.

Fig. 4 shows system performance with a time-varying ambient noise level, consisting of a slowly varying component and a white noise component. The seabed is flat at depth $150\,\mathrm{m}$. One can notice how the formation scale γ follows some trends that mirror the changes in the SNR levels (in the sense that γ increases when the SNR increases too). As in the previous case, the timeseries associated to γ exhibit some ripples.

Fig. 5 shows system performance in a realistic scenario with a time-varying ambient noise level, white noise, and a variable sea depth. We can note how the variation of γ is not explainable anymore just with the variation of the SNR associated to the acoustic channel. For instance note in the interval $t \in [3000, 4000]$ that the value of γ decreases, even if the SNR increases.

As is clear from Figs. 3, 4, and 5, there are some oscillation present in the formation scale. As mentioned previously, this is mostly due to insufficient bandwidth separation between the formation scaling and threshold adjustment algorithms. The issue is further amplified by the long moving average filters introduced to both algorithms to minimize the impact of the occasional spikes in packet loss. This is problematic, however one may also observe in Fig. 5 that the algorithm struggles to keep up with the fast changes

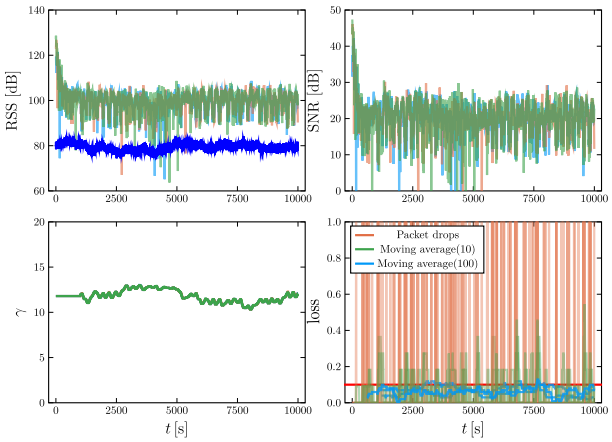

Fig. 4. Example of the system performance under the simulated environment case 2 (flat seabed and time varying noise level) with 3 agents, shown in light blue, orange, and green respectively. The top left panel shows the received signal strength (RSS) as well as the noise level in dark blue, the top right shows the SNR, the formation scale γ, and the bottom right shows packet losses, as well as moving average estimates of the packet loss with window sizes 10 and 100. The desired packet loss of 10% is marked in red.

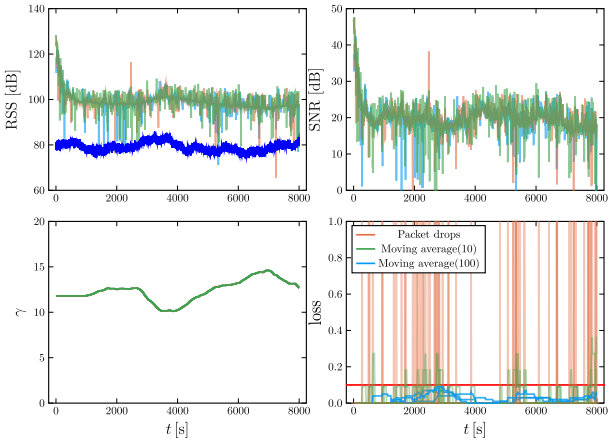

Fig. 5. Example of the system performance under the simulated environment case 3 (non-flat seabed and time varying noise levels) with 3 agents, shown in light blue, orange, and green respectively. The top left shows the received signal strength (RSS) as well as the noise level in dark blue, the top right shows the SNR, the formation scale γ, and the bottom right shows packet losses as well as moving average estimates of the packet loss with window sizes 10 and 100. The desired packet loss of 10% is marked in red.

in the communication conditions, indicating that there is a tradeoff between quick reactivity to environmental changes, and stabilizing the influence of bursts of lost packets.

It is clear that the consensus algorithms are sensitive to packet loss. This means that in order to stabilize the estimates of e.g. the formation barycenter, the desired packet loss should be kept low. This is usually suitable, as the bandwidth of acoustic communications is fairly low, meaning that it is desirable to maximize the uptime of the acoustic link.

The proposed method only considers movements in the plane. While this is relevant in the sense that many underwater systems need to maintain certain depths or distances from the seabed, it is worth noting that due to the nature of underwater sound propagation, significant changes to the incoming SNR can be achieved with relatively small vertical movements. This does however lead to higher needs for coordination of the AUVs.

VI. Conclusions and Future Work

We have presented a method for dynamically scaling a formation of AUVs according to the quality of the communication, so to stabilize an estimated packet loss probability at a desired level l_d all while using minimal communication bandwidth. This method has been verified with high-fidelity acoustic simulations. Simulations in a simplified environment with a flat seabed show that the algorithm is able to stabilize the scaling of the formation at a suitable level under static conditions. Further tests with a varying ambient noise level show that the algorithm is able to adjust the scale to stabilize the communication packet loss. Finally, simulations in a more realistic scenario with both a varying noise level and bathymetry show that the algorithm is also able to constrain the packet loss under such dynamic conditions.

The challenges associated with the method are associated with the tuning of its parameters, which if performed improperly may imbalance its responsiveness (i.e., the time it takes to react to changing conditions) versus its ability to tolerate bursts of packet losses or in general moments where reception is more difficult. Ideally one would also like the parameters of such an algorithm to be adaptive; this meta-controller is thus a potential future work.

Other future works may aim at relaxing the requirement of planar movements to also leverage possible improvements by vertical movement.

References

[1] F. Arrichiello, S. Chiaverini, and T. I. Fossen, "Formation control of underactuated surface vessels using the null-space-based behavioral control," in *Proc. 2006 IEEE/RSJ International Conference on Intelligent Robots and Systems*, pp. 5942–5947, 2006.

[2] G. Antonelli, F. Arrichiello, and S. Chiaverini, "Experiments of formation control with multirobot systems using the null-space-based behavioral control," *IEEE Transactions on Control Systems Technology*, vol. 17, no. 5, pp. 1173–1182, 2009.

[3] S.-k. Pang, Y.-h. Li, and H. Yi, "Joint formation control with obstacle avoidance of towfish and multiple autonomous underwater vehicles based on graph theory and the null-space-based method," *Sensors*, vol. 19, no. 11, 2019.

[4] J. Matouš, K. Y. Pettersen, and C. Paliotta, "Formation path following control of underactuated AUVs," in *Proc. 2022 European Control Conference*, 2022.

[5] J. Matouš, K. Y. Pettersen, D. Varagnolo, and C. Paliotta, "Singularity-free formation path following of underactuated AUVs," in *Proc. 2023 IFAC World Congress*, 2023.

[6] J. Matouš, K. Y. Pettersen, D. Varagnolo, and C. Paliotta, "A distributed NSB algorithm for formation path following," *Submitted to IEEE Transactions on Control Systems Technology*, 2023. pre-print available at `https://www.dropbox.com/s/3as1c4pmq90yavy/SubmittedVersion.pdf?dl=0`.

[7] P. Qarabaqi and M. Stojanovic, "Statistical characterization and computationally efficient modeling of a class of underwater acoustic communication channels," *IEEE Journal of Oceanic Engineering*, vol. 38, no. 4, pp. 701–717, 2013.

[8] H. Schmidt and T. Schneider, "Acoustic communication and navigation in the new arctic — a model case for environmental adaptation," in *Proc. 2016 IEEE Third Underwater Communications and Networking Conference (UComms)*, pp. 1–4, 2016.

[9] M. Chitre and L. Kexin, "Physics-informed data-driven communication performance prediction for underwater vehicles," in *Proc. 2022 Sixth Underwater Communications and Networking Conference (UComms)*, 2022.

[10] W. Cao, J. Yan, X. Yang, X. Luo, and X. Guan, "Communication-aware formation control of auvs with model uncertainty and fading channel via integral reinforcement learning," *IEEE/CAA Journal of Automatica Sinica*, vol. 10, no. 1, pp. 159–176, 2023.

[11] N. DiLeo, A. Abad, and K. Pregene, "Communications aware decentralized model predictive control for path planning within uuv swarms," in *Proc. 2017 IEEE Conference on Control Technology and Applications (CCTA)*, pp. 249–254, 2017.

[12] G. Antonelli, F. Arrichiello, and S. Chiaverini, "Stability analysis for the null-space-based behavioral control for multi-robot systems," in *Proc. 47th IEEE Conference on Decision and Control*, 2008.

[13] D. Belleter, M. A. Maghenem, C. Paliotta, and K. Y. Pettersen, "Observer based path following for underactuated marine vessels in the presence of ocean currents: A global approach," *Automatica*, vol. 100, pp. 123–134, 2019.

[14] D. Deplano, M. Franceschelli, and A. Giua, "Dynamic min and max consensus and size estimation of anonymous multiagent networks," *IEEE Transactions on Automatic Control*, vol. 68, no. 1, pp. 202–213, 2023.

[15] M. Franceschelli and A. Gasparri, "Multi-stage discrete time dynamic average consensus," in *Proc. 2016 IEEE 55th Conference on Decision and Control (CDC)*, pp. 897–903, 2016.

[16] M. Chitre, "Underwater acoustics in the age of differentiable and probabilistic programming," 2020. `https://org-arl.github.io/UnderwaterAcoustics.jl/v0.1/`.